Materials Discovery 1 (2015) 2–9

Contents lists available at ScienceDirect

Materials Discovery

journal homepage: www.elsevier.com/locate/md

Identification of peptide adsorbates for strong nanoparticle–nanoparticle binding by lattice protein simulations

Daniel M. Packwood [a,*], Kazuto Akagi [a], Mitsuo Umetsu [b,a]

[a] Advanced Institute for Materials Research, Tohoku University, 2-1-1 Katahira, Aoba-ku, Sendai 980-8577, Japan
[b] Department of Biomolecular Engineering, Graduate School of Engineering, Tohoku University, 6-6-11 Aoba, Aramaki Aoba-ku, Sendai 980-8579, Japan

ARTICLE INFO

Article history:
Received 4 August 2015
Received in revised form 28 October 2015
Accepted 30 October 2015
Available online 19 December 2015

Keywords:
Nanoparticle
Surface
Protein
Peptide
Lattice protein
Monte Carlo

ABSTRACT

Nanoparticles with short peptides adsorbed to their surfaces often assemble into interesting structures when suspended solution. In this paper, the interaction between a peptide adsorbed to a surface and another peptide adsorbed to an opposing surface is studied using the lattice protein model. It is found that the interaction strength between the two peptides generally increases as the hydrophobicity of peptides increases. Moreover, there is a preference for hydrophobic amino acids to be neighboring hydrophilic amino acids in cases which yield strong peptide–peptide interactions. These results provide insights for tailoring the strength of nanoparticle–nanoparticle binding by engineering of peptide adsorbates.

1. Introduction

Metal and inorganic nanoparticles have received extensive attention as possible building blocks for novel nanotechnologies [1]. While nanoparticles usually assemble into amorphous coagulates when suspended in solution [2], nanoparticles with organic molecules or short (∼10-mer) peptides adsorbed to their surfaces often assemble into structures with interesting shapes and properties [2–7]. The result of this assembly depends on which parts of the nanoparticle surface the adsorption takes place [6], the molecular structure and surface selectivity of the adsorbate [8,9], the experimental conditions (temperature, pressure, pH, and solvent) under which the assembly process is performed [10], and the strength of the interaction between molecules adsorbed to opposing nanoparticle surfaces. By analogy with chemical bonding between atoms, it is possible to speak of the connection formed between two nanoparticles *via* surface-adsorbed peptides as a 'nanoparticle–nanoparticle bond'. However, while the fundamentals of chemical bonding are well-understood, the general principles that connect the chemical composition of the adsorbate molecules with the strength of the nanoparticle–nanoparticle bond remain unknown.

This paper considers the interaction between two short peptides adsorbed to two opposing surfaces as a model for the nanoparticle–nanoparticle bond described above. While this exact situation does not appear to have been studied in the literature, peptide adsorption to a single surface has been investigated thoroughly, especially from the point-of-view of biomedical applications [11–17]. It is now well-accepted that peptides adsorbed to surfaces have quite a different equilibrium structure than peptides in the gas- or liquid phase [14,18,19] and the kinetics of this adsorption process has been characterized with rate equations for a variety of cases [14,16,17]. The adsorption strength is also highly dependent on the amino acid sequence of the peptide [8]. These studies are proceeding toward a microscopic understanding of surface-adsorbed and confined peptides, however there remains the outstanding practical problem of identifying peptide sequences to achieve a strong nanoparticle–nanoparticle bond.

In this paper, the interaction between two peptides adsorbed to opposing surfaces is considered from the point-of-view of the lattice protein model (Fig. 1) [20]. We investigate how the amino acid sequence of the peptide affects the strength of the nanoparticle–nanoparticle bond, as measured by the interaction strength between the two peptides. The lattice protein model is an early model for protein folding [21,22] and continues to be used extensively to study protein physics [23–28]. This model treats the peptide as a string of beads, where each bead is a single amino acid. The beads reside on vertices of a cubic lattice, and

* Corresponding author. Tel.: +81 0222176149.
E-mail address: packwood@wpi-aimr.tohoku.ac.jp (D.M. Packwood).

http://dx.doi.org/10.1016/j.md.2015.10.003
2352-9245/

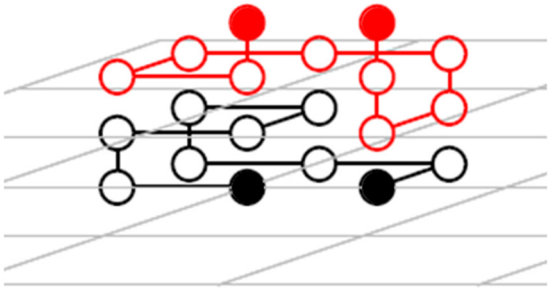

Fig. 1. Lattice protein model for the nanoparticle–nanoparticle bond. The gray grid represents the lower surface. The upper-surface is not shown. The two filled black beads are fixed to the lower surface, and the two filled red beads are fixed to the upper-surface.

only interactions between beads on adjacent sites of the cubic lattice contribute to the total energy of peptide. The lattice protein model is obviously inappropriate for predicting the detailed conformation of real peptides, however it is surprisingly successful at correlating the equilibrium stability with peptide amino acid sequence [29]. The lattice protein model has been used to study adsorption of single peptides to single surfaces [30] and between surfaces [31]. With the availability of detailed atomistic molecular dynamics (MD) simulations and quantum chemical calculations, it may seem unnecessary to resort to the lattice protein model at all. On the other hand, atomistic MD simulations are only useful with a force field which accounts for both the metal surface–amino acid and amino acid–amino acid interactions with the same level of accuracy. Such force fields are only just starting to appear in the literature and are restricted to specific metal surfaces [32–35]. In contrast, surface-amino acid interactions can be incorporated into the lattice protein model as a set of free parameters, which provides generality in the kind of surfaces that can be studied. This fact, as well as the relative computational efficiency of scanning large libraries of peptide sequences with the lattice protein model, makes the lattice protein model a very reasonable approach for identifying optimal peptides for strong nanoparticle–nanoparticle bonding. We will consider a special case where the terminal amino acids of the peptides are immobile and in direct contact with their respective surfaces. The situation might be relevant to the case of cysteine-terminated peptides adsorbed to gold nanoparticles [36].

Via Monte Carlo simulations on an extensive library of randomly generated, 10-mer peptides, we find that in general the strength of the nanoparticle–nanoparticle bond (as measured by the peptide–peptide interaction energy) tends to increase as the fraction of hydrophobic amino acids in the peptide increases, and tends to decrease as the fraction of hydrophilic amino acids in the peptide increases. These trends become more dramatic as the hydrophilicity of the surface increases. These results resemble the general rule-of-thumb that isolated peptides in aqueous environments tend to fold in such a way that their hydrophobic amino acids are buried within the core of the folded protein and can interact with each other [37,38]. Unexpectedly, we find that in peptides which lead to strong nanoparticle–nanoparticle bonding, hydrophobic amino acids are often neighboring hydrophilic or mildly hydrophobic amino acids. This may facilitate the interaction between the two peptides by preventing the peptides from 'folding into themselves' and not interacting with each other. This preference for hydrophobic–hydrophilic pairing becomes weaker as the surface hydrophilicity increases, but nonetheless still appears important in peptides which yield strong nanoparticle–nanoparticle bonding. These results therefore provide, for the first time, a starting point for tuning the strength of the nanoparticle–nanoparticle bond by careful engineering of the peptide surface adsorbates.

This paper is organized as follows. Section 2 describes the lattice protein model and the Monte Carlo simulation technique utilized here to calculate the interaction strength between the two peptides. Section 3 presents our main results and a detailed discussion, and conclusions are left for Section 4.

2. Methods

We consider two lattice proteins adsorbed to two opposing surfaces (Fig. 1). Each protein is modeled as a string of beads, where each bead represents an amino acid [20–22]. The beads occupy vertices of a cubic lattice and are labeled as 1, 2,..., where the numbering starts at one of the terminal residues. Henceforth we will refer to these beads as amino acids. The lower (upper) surface is denoted by S_1 (S_2), and the peptide adsorbed to S_1 (S_2) is denoted by P_1 (P_2). All configurations of the model must satisfy the following two conditions: the two terminal amino acids of P_1 (P_2) are always fixed to S_1 (S_2); no two amino acids may occupy the same vertex of the lattice; and no amino acid may reside at vertices below S_1 or at vertices above S_2. The first condition is expected to be satisfied for the case of cysteine-terminated peptides adsorbed to gold surfaces [36]. Consider some configuration for the model σ that satisfies these conditions and let $P_k(\sigma)$ denote peptide k when the model is in this configuration. The energy of configuration σ is defined as

$$\varepsilon(\sigma) = \sum_{\{i\sim j: i,j\in P_1(\sigma)\}} \varepsilon_{ij} + \sum_{\{i\sim j: i,j\in P_2(\sigma)\}} \varepsilon_{ij} + \sum_{\{i\sim j: i\in P_1(\sigma), j\in P_2(\sigma)\}} \varepsilon_{ij} + \sum_{\{i\sim S_1\}} u_i + \sum_{\{i\sim S_2\}} u_i \quad (1)$$

where the notation $\{i\sim j : i,\ j\in P_m(\sigma)\}$ denotes all pairs (of non-covalently bonded) amino acids which are contained in peptide $P_m(\sigma)$ and reside at adjacent vertices on the cubic lattice, $\{i\sim j : i\in P_m(\sigma),\ j\in P_n(\sigma)\}$ denotes all pairs of amino acids which reside at adjacent vertices on the cubic lattice such that amino acid i is contained in peptide $P_m(\sigma)$ and amino acid j is contained in peptide $P_m(\sigma)$, and $\{i\sim S_k\}$ denotes all amino acids that are adjacent to surface S_k. In Eq. (1), ε_{ij} is the interaction energy between amino acids i and j, and u_i is the interaction energy between amino acid i and the surface. Note that the interaction between amino acids which are covalently bonded does not contribute to Eq. (1). The probability that configuration σ occurs at equilibrium is

$$g(\sigma) \propto \exp\left(\frac{-\varepsilon(\sigma)}{k_B T}\right) \quad (2)$$

where k_B is the Boltzmann constant and T the temperature. The normalizer constant (partition function) in Eq. (2) is assumed to be unknown. The task of this paper is to estimate the *peptide–peptide interaction energy*, defined as

$$E_{\text{int}} = \langle \varepsilon_{\text{int}}(\sigma) \rangle, \quad (3)$$

where

$$\varepsilon_{\text{int}}(\sigma) = \sum_{\{i\sim j: i\in P_1(\sigma), j\in P_2(\sigma)\}} \varepsilon_{ij} \quad (4)$$

is the protein–protein interaction energy when the model is in configuration σ, and the angular brackets denotes an average with respect to the probability distribution $g(\sigma)$ in Eq. (2).

In this paper, we estimate (3) *via* MCMC sampling with the Metropolis-Hastings algorithm. For an introduction to this technique, the reader is referred to literature sources [39,40]. In order to scan the configuration space of the model during the MCMC sampling, we employ *shift transformations*. An individual shift transformation on amino acid l of peptide k in the direction x,

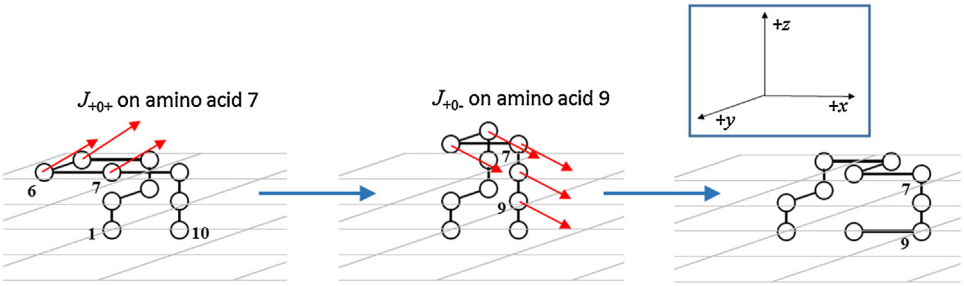

Fig. 2. Example of the shift transformations $J_{+0+}{}^{17}$ and $J_{+0-}{}^{19}$. The axis labeling conventions are shown in the insert.

y, z, is denoted by J^{kl}_{xyz}. With reference to Fig. 2, the shift transformation $J^{1,7}_{+0+}$ on amino acid 7 of peptide 1 runs as follows. (i) Following the labeling convention for the axes shown in the insert of Fig. 2, an arrow is drawn starting at amino acid 7 of protein P_1 pointing in the positive x direction and the positive z direction. (ii) The amino acid that is connected to amino acid 7 and does not fall under the projection of the arrow drawn in step (i) is identified. In Fig. 2, this is residue number 6. (iii) An arrow starting at residue 6 pointing in the positive x direction and positive z direction is drawn. (iv) Arrows on amino acids 5, 4, and so on are drawn until we reach a residue m that falls under the projection of the arrow on amino acid $m+1$. In Fig. 2, $m=4$. Then, the amino acids 7, 6, and 5 are shifted the direction of these arrows. In this paper, we employ the shift transformations $J^{kl}_{+0-}, J^{kl}_{-0-}, J^{kl}_{-0+}, J^{kl}_{+0+}, J^{kl}_{0--}, J^{kl}_{0++}, J^{kl}_{0+-}, J^{kl}_{0-+}, J^{kl}_{++0}, J^{kl}_{+-0}, J^{kl}_{--0}$, and J^{kl}_{-+0}. The shift transformations are closely related to the 'pull' transformations used by other authors [31,41]. Shift transformations are less localized than pull transformations and tend to reduce the 'compactness' [22] of the peptide, which is preferable when studying peptides adsorbed to interfaces [30]. In the Metropolis-Hastings algorithm, the probability of making a transition from configuration σ to configuration σ' is set to be

$$q(\sigma, \sigma') = \frac{N_{\sigma,\sigma'}}{N_\sigma}, \tag{5}$$

where N_σ is the total number of shift transformations that are possible when the model is in configuration σ, and $N_{\sigma,\sigma'}$ is the number of those configurations that result in the configuration σ'. The MCMC sampling procedure was supplemented with parallel tempering to improve the rate of convergence of the MCMC algorithm [42]. This was implemented with 15 replicas with temperatures 298 K, 348 K, 398 K, . . ., 948 K and 998 K, respectively. All results reported here were calculated at 298 K, which is the relevant temperature for nanomaterials design *via* surface-modified nanoparticles. A script for performing these calculations was written for *R* [43,44] and is available as Supporting Information.

3. Results and discussion

The following calculations used the parameters shown in Table 1a with random initial configurations. The amino acid–amino acid interaction energies ε_{ij} were assigned according to the Miyazawa–Jernigan force field (see Table SA of the Supporting Information or Table 3 of Ref. [45]). In order to assign the surface-amino acid interaction energies, we distinguish three categories of amino acid, namely 'hydrophobic', 'mildly hydrophobic', and 'hydrophilic' (Table 1a). The surface-amino acid interaction energy for amino acid u_i is then set to $\varepsilon_{hydrophobic}$ (respectively ε_{mild}, $\varepsilon_{hydrophilic}$) if the amino acid is classified as hydrophobic (respectively midly hydrophobic, hydrophilic). While the interaction between several amino acids and several specific surfaces has been studied in detail [46–50], we are without a complete set of surface-amino acid interaction parameters for use in the lattice protein model. We therefore consider several artificial regimes for the parameters $\varepsilon_{hydrophobic}$, ε_{mild}, and $\varepsilon_{hydrophilic}$ as described in Table 1b. These regimes cover a wide range of possible hydrophilicities for a nanoparticle surface. MCMC sampling as described above was performed under each of these parameter regimes for 500 randomly generated, cysteine-terminated peptide sequences containing 10 amino acids, and the interaction energy E_{int} was estimated for each case using Eq. (9). Note that cysteine amino acids were not permitted to appear between the terminals when generating these peptides. The MCMC sampling procedures were ran for 100,000 steps, and the first 10,000 steps were dropped when calculating E_{int}. This criterion was chosen after comparison with several trial simulations of 200,000 steps, each with E_{int} calculated by dropping the first 70,000 steps. These simulations showed no qualitative difference with the results reported here. In the following discussion, we will focus exclusively on the case of an inert surface, which serves as a baseline case, and on the case of a strongly hydrophilic surface, which is most relevant for peptides which are strong adsorbed to gold surfaces *via* cysteine terminal residues. Data for the other cases described in Table 1b can be found in the Supporting Information.

3.1. Inert surface case

We first consider the 'baseline' case of an inert surface as described in Table 1b. Fig. 3 plots the peptide–peptide interaction energy E_{int} estimated from the 500 peptide sequences as a function of the number of hydrophobic amino acids, number of

Table 1
(A) Classification of amino acids. (B) Parameters for the surface-amino acid interaction. Energies are in units of *RT*, where *R* is the gas constant and *T* is 298 K.

(A)

Hydrophobic	I (Ile), F (Phe), V (Val), L (Leu), M (Met)
Mildly hydrophobic	W (Trp), A (Ala), G (Gly), C (Cys), Y (Tyr), P (Pro), T (Thr), S (Ser)
Hydrophilic	H (His), E (Glu), N (Asn), Q (Gln), D (Asp), K (Lys), R (Arg)

(B)

Parameter regime	Surface–hydrophobic amino acid (*RT*)	Surface-mildly hydrophobic amino acid (*RT*)	Surface–hydrophilic amino acid (*RT*)
Strongly hydrophobic surface	−6.00	−3.00	−2.25
Mildly hydrophobic surface	−3.00	−1.50	−0.75
Inert surface	0.00	0.00	0.00
Weakly hydrophilic surface	−0.10	−0.25	−0.50
Mildly hydrophilic surface	−0.25	−0.50	−1.00
Strongly hydrophilic surface	−0.75	−1.50	−3.00

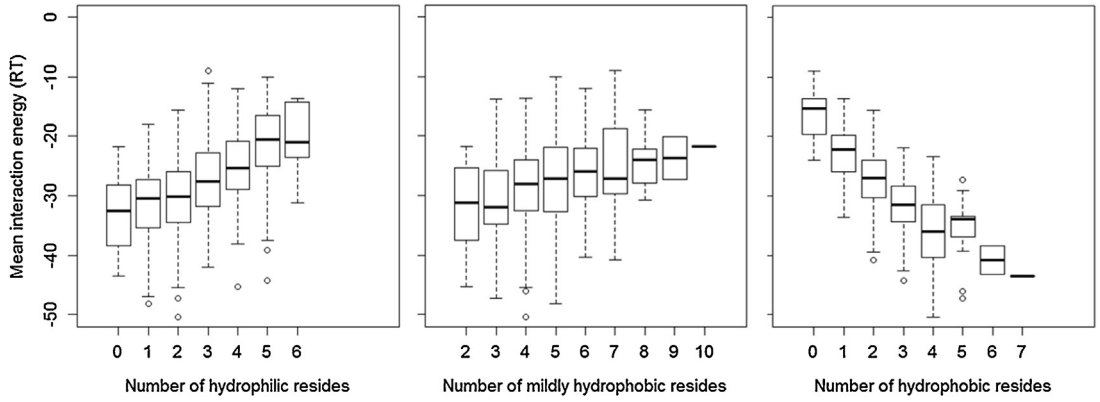

Fig. 3. Box-and-whisker plots of the interaction energy E_{int} of 500 randomly generated peptides (inert surface case). Energy is measured in units of *RT*, where *R* is the gas constant and *T* is 298 K.

mildly hydrophobic acids, and number of hydrophilic amino acids in the peptide. It can be seen that, on average, the interaction strength strongly increases (E_{int} tends to decrease) as the number of hydrophobic amino acids increases in the protein, weakly decreases as the number of mildly hydrophobic amino acids increases in the peptide, and strongly decreases as the number of hydrophilic amino acids increases in the peptide. These observations are sensible, as free proteins in solution (not in the vicinity of any surface) often fold such that their hydrophobic amino acids are buried within a 'hydrophobic core' and their hydrophilic amino acids are exposed to the outside solution [37,38].

The plots in Fig. 3 show that the overall number of hydrophobic amino acids in the peptide are important for determining the strength of the peptide–peptide interaction, however they do not provide any insight into the role of the *local* amino acid sequence in this interaction. To collect such local information, we identified the 10 peptide sequences that yielded the strongest peptide–peptide interaction, and then identified all neighboring pairs of amino acids that occur in these peptides. Table 2a lists all neighboring pairs of amino acids which appeared at least two times in this analysis. It can be seen that most pairs involve one hydrophobic amino acid and one mildly hydrophobic or hydrophilic amino acid. This would suggest that, while having hydrophobic amino acids in the peptide is important for obtaining strong peptide–peptide interactions, it is important for these amino acids to be neighboring mildly hydrophobic or hydrophilic amino acids. This unexpected result is not obvious from Fig. 3 alone. From a chemical point-of-view, it appears preferable for the hydrophobic amino acids in these pairs to bear aromatic side-chains, as is implied by the large number of times F appears in these pairs. Three does not appear be any particular preference for any type of side-chain in the hydrophilic amino acids in these pairs, due to the variety of hydrophilic amino acids that appear in these pairs, including amino acids that engage in hydrogen bonding (such as S), and charged amino acids (such as K and R). This information may be useful for engineering peptides which lead to strong nanoparticle–nanoparticle bonds. While it is unclear how appropriate the lattice protein model is for predicting specific sequences for achieving strong nanoparticle–nanoparticle bonding, the specific amino acid pairs that appear in Table 2a might nonetheless serve as useful starting points for engineering peptides which yield strong nanoparticle–nanoparticle bonds.

Table 2a
Neighboring pairs of amino acids that occur more than once in the ten peptides with strongest nanoparticle–nanoparticle bonding (inert surface case). 'Number' refers to the number of times the pair was observed. 'Type' refers to the hydrophobicity of the amino acid; *x* = hydrophobic, *y* = mildly hydrophobic, *z* = hydrophilic. The number in brackets refers to the number of times the 'type' of pair occurs (*e.g.*, for first row, 4 (6) means that the amino acid pair F and I appeared four times in the analysis, and (6) means that amino acids pairs of type *x* and *x* appeared 6 times in total).

Pair		Type		Number
F	I	*x*	*x*	4 (6)
L	K	*x*	*z*	3 (16)
R	F	*z*	*x*	3
F	S	*x*	*y*	3 (12)
W	M	*y*	*x*	3
F	K	*x*	*z*	3
N	I	*z*	*x*	3
S	W	*y*	*y*	2 (2)
P	F	*y*	*x*	2
F	T	*x*	*y*	2
F	G	*x*	*y*	2
I	L	*x*	*x*	2
F	H	*x*	*z*	2
L	E	*x*	*z*	2
R	H	*z*	*z*	2 (2)

The appearance of alternating hydrophobic–hydrophilic pairs may prevent the peptides from 'folding into themselves' and not interacting with the peptide on the opposite surface. First, note that the interaction between hydrophobic amino acids is typically much stronger than the interaction between hydrophilic amino acids. For example, in the case of the Miyazawa–Jernigan force field [45], the interaction energy between two hydrophobic F amino acids is −7.26 *RT* whereas the interaction energy between two hydrophilic N amino acids is −1.67 *RT*. Now, consider the 4-mer $X_1X_2X_3X_4$, where the X's denote hydrophobic amino acids. In this case, it is possible for the 4-mer to fold into a stable conformation such that that amino acids X_1 and X_4 are adjacent. The peptide would then spend less exploring the region between the two surfaces and interacting with the peptide on the opposite surface, due to the energy barrier needed to break the hydrophobic–hydrophobic interactions within the peptide. On the other hand, the 4-mer $X_1Y_2X_3Y_4$, where the Y's are hydrophilic amino acids, cannot fold into a conformation such that the hydrophobic amino acids X_1 and X_3 are adjacent and interacting. This peptide might be expected to spend more time exploring the region between the two surfaces and interacting with the peptide on the opposite surface, as the energy barrier needed to break the hydrophobic–hydrophilic interactions within a single peptide are relatively small. This explanation is supported by Table S3.3 of the Supporting Information, which show that in the peptides which yield the strongest nanoparticle–nanoparticle bonding, the third nearest neighbor combinations tend to be of the type X_1Y_4 rather than X_1X_4, where the X's denote hydrophobic amino acids and the Y's denote hydrophilic or mildly hydrophobic amino acids.

We now consider neighboring pairs of amino acids which occur in sequences with very weak peptide–peptide interactions. Table 2b lists all neighboring amino acids that appeared in the 10 peptides with the weakest peptide–peptide interactions. Similar to

Table 2b
Neighboring pairs of amino acids that occur more than once in the ten peptides with weakest nanoparticle–nanoparticle bonding (inert surface case). 'Number' refers to the number of times the pair was observed. 'Type' refers to the hydrophobicity of the amino acid; x = hydrophobic, y = mildly hydrophobic, z = hydrophilic.

Pair		Type		Number
A	P	y	y	5 (13)
G	K	y	z	5 (27)
T	Q	y	z	3
Q	D	z	z	3 (5)
P	S	y	y	3
T	P	y	y	3
R	T	z	y	3
A	N	y	z	2
R	S	z	y	2
S	T	y	y	2
D	S	z	y	2
A	K	y	z	2
S	K	y	z	2
P	R	y	z	2
A	Q	y	z	2
D	P	z	y	2
K	H	z	z	2

Table 3a
Neighboring pairs of amino acids that occur more than once in the ten peptides with strongest nanoparticle–nanoparticle bonding (strong hydrophilic surface case). 'Number' refers to the number of times the pair was observed. 'Type' refers to the hydrophobicity of the amino acid; x = hydrophobic, y = mildly hydrophobic, z = hydrophilic.

Pair		Type		Number
F	T	x	y	5 (22)
F	L	x	x	4 (13)
F	I	x	x	3
T	L	y	x	3
L	A	x	y	3
P	F	y	x	3
L	L	x	x	2
L	M	x	x	2
M	F	x	x	2
F	R	x	z	2 (4)
R	S	z	y	2 (2)
G	F	y	x	2
R	M	z	x	2
M	T	x	y	2
V	A	x	y	2
T	I	y	x	2

the results described above, we often find that the neighbors occur in pairs of hydrophilic and mildly hydrophobic amino acids. Pairs containing hydrophobic amino acids do not appear in Table 2b. The occurrence of hydrophilic-mildly hydrophobic amino acid neighbors in Table 2b may be due to a mechanism similar to the one described above; namely that the mildly hydrophobic amino acids may increase the stability of configurations where the two peptides are 'folded into themselves' and have only few contacts with the other peptide. However, it should be noted that the preference for pairs of hydrophilic and mildly hydrophobic amino acids in this case is not as strong as the preference for pairs of hydrophobic and mildly hydrophobic amino acids described above for the case of peptides with strong peptide–peptide interactions. In particular, there are several occurrences of hydrophilic–hydrophilic and mildly hydrophobic-mildly hydrophobic amino acid neighbor pairs for the present case. This result suggests that the local hydrophilicity and overall hydrophilicity are both important for achieving weak nanoparticle–nanoparticle bonding. A variety of chemical side chains appear in the amino acids in Table 2b, including side chains that undergo hydrogen bonding (such as in T, and S), charged side chains (such as in K, D, R), and relatively non-polar side chains (such as in A and G), and there does not appear to be any preference for any particular side chain chemistry in Table 2b. This observation further suggests that it is the overall hydrophilicity of the peptide, rather than the particular amino acids which appear in the peptide, which determine the weakness of the peptide–peptide interaction.

3.2. Strongly hydrophilic surface

Fig. 4 plots the interaction energies E_{int} estimated from the 500 peptide sequences as a function of the number of hydrophobic amino acids, number of mildly hydrophobic acids, and number of hydrophilic amino acids in the peptide, for the case of a strongly hydrophilic surface. The trends observed in Fig. 4 are qualitatively the same as in Fig. 3, however now the mean interaction energies decrease more dramatically on average as the number of hydrophilic amino acids increases in the protein, and increase more dramatically as the number of hydrophilic amino acids decrease in the chain. Interestingly, there appears to be a step-decrease of about 15 RT (on average) in the interaction strength upon going from 5 to 6 hydrophilic amino acids in the peptide, and upon going from 6 to 7 hydrophilic residues, the mean interaction energy is essentially zero for all peptide sequences tested. While the variation in the interaction strength is particularly large for peptides with 5 and 6 hydrophilic amino acids, it nonetheless appears that there is a transitionary behavior in the interaction strength across the range of 4–7 hydrophilic amino acids. This suggests that the nanoparticle–nanoparticle bond strength may suddenly decrease as the fraction of hydrophilic amino acids in the peptide changes by a small amount. Note that the negligibly small variance in interaction strengths for peptides with 7 hydrophilic amino acids may be artificial due to the relatively small number of peptides with 7 hydrophilic amino acids which appeared in our random sample.

Table 3a lists pairs of amino acids which occurred in the ten peptide sequences with the strongest peptide–peptide interactions. As was observed in the case of an inert surface, hydrophobic amino acids paired with mildly hydrophobic or hydrophilic amino acids feature extensively in the list. However, we also see the appearance of several hydrophobic–hydrophobic pairs, which suggests a weaker preference for hydrophobic–hydrophilic and hydrophobic-mildly hydrophobic pairing for the case of a hydrophilic surface. In terms of the mechanism described for the inert surface case, it may be that peptides with alternating hydrophobic and hydrophilic amino acid pairs are liable to 'stick' to their respective surfaces and not interact with the peptide on the other surface; on the other hand, if the amino acids of the peptides did not alternate in this fashion, then the peptide would possess well-defined hydrophobic and hydrophilic regions. The hydrophilic regions would then tend to stick to the surface, and the hydrophobic regions would tend to extend into the space between the surfaces and interact with the other peptide. Apart from this observation, the trends seen in Table 3a are qualitatively the same as those described in Table 2a. In particular, F again features heavily on this list, again suggesting some preference for amino acids with aromatic side chains in peptides with strong peptide–peptide interactions, however the preference does not appear as strong as in the case of an inert surface, as we also see several hydrophobic amino acids with non-aromatic side chains as well (such as in L, I, and G). Similarly to the case of an inert surface, there does not appear to be any particular preference for side chain chemistry for the hydrophilic or mildly hydrophobic partner in the pair, as a variety of side-chain chemistries appear in these amino acids in Table 3a (such as the amino acid T, whose side chain which participate in hydrogen bonding, and the amino acid R, whose side chain is charged).

Table 3b lists neighboring pairs of amino acids that occurred in the ten peptides with the weakest peptide–peptide

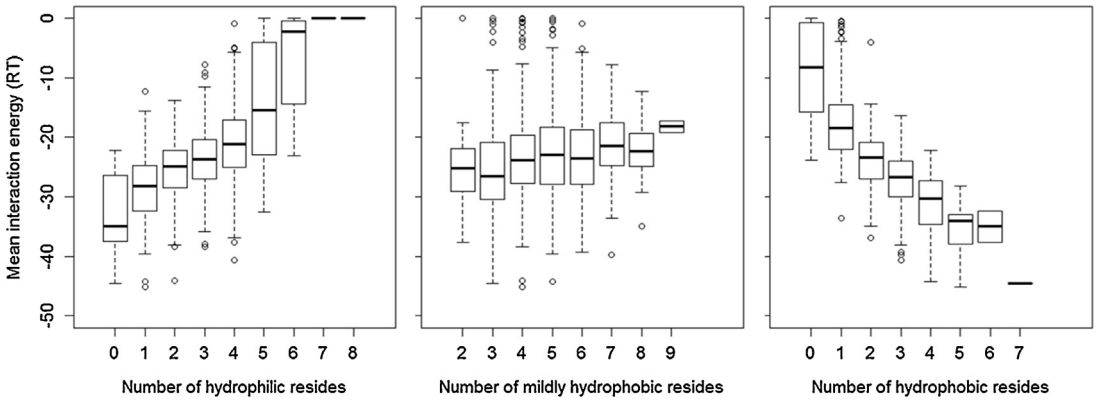

Fig. 4. Box-and-whisker plots of the interaction energy E_{int} of 500 randomly generated peptides (strongly hydrophilic case).

Table 3b
Neighboring pairs of amino acids that occur more than once in the ten peptides with weakest nanoparticle–nanoparticle bonding (hydrophilic surface case). 'Number' refers to the number of times the pair was observed. 'Type' refers to the hydrophobicity of the amino acid; *x* = hydrophobic, *y* = mildly hydrophobic, *z* = hydrophilic.

Pair		Type		Number
E	R	*z*	*z*	5 (30)
E	N	*z*	*z*	5
H	E	*z*	*z*	3
K	H	*z*	*z*	3
N	P	*z*	*y*	3 (11)
R	K	*z*	*z*	2
R	H	*z*	*z*	2
Q	R	*z*	*z*	2
K	A	*z*	*y*	2
A	N	*y*	*z*	2
S	Q	*y*	*z*	2
D	S	*z*	*y*	2
A	T	*y*	*y*	2 (2)
E	K	*z*	*z*	2
K	K	*z*	*z*	2
E	E	*z*	*z*	2
N	K	*z*	*z*	2

interaction for the strongly hydrophilic surface case. In comparison to the inert surface case (Table 2b), we see a clear preference for hydrophilic–hydrophilic pairs in peptides with weak peptide–peptide interaction strength, with relatively few pairs containing mildly hydrophobic amino acids. No pair in Table 2b contains a hydrophobic amino acid. Moreover, there is a clear abundance of amino acids with charged side chains in Table 3b (such as E, R, and H), which demonstrates a much stronger preference for charged side chains for achieving weak peptide–peptide interactions in the present case compared with the inert surface. Amino acids which charges tend to have very weak interactions with other charged amino acids (in the Miyazawa–Jernigan force field, the interaction energy between two the charged amino acids R interaction is only −0.91 *RT*, for example [45]), and thus peptides containing many charged amino acids can only ever be expected to interact weakly with themselves and each other. It is therefore very reasonable that such peptides would stabilize by maximizing their contact with their respective hydrophilic surfaces rather than with each other, and thereby yielding weak nanoparticle–nanoparticle bonds.

4. Conclusions

By simulations of the lattice protein model for a large library of randomly generated peptide sequences, we have investigated the problem of choosing peptide adsorbates for metal nanoparticle surfaces which lead to strong 'nanoparticle–nanoparticle bonding' between nanoparticles. Under the conditions employed in the simulation, our predictions are expected to be most relevant to the case of cysteine-terminated peptides adsorbed to gold metal nanoparticle surfaces, in which the cysteine amino acids chemisorb to the surface and stay fixed thereafter [36]. It was found that in general, the strength of the nanoparticle–nanoparticle bond (measured by the interaction energy between peptides adsorbed to opposing surfaces) increases as the fraction of hydrophobic amino acids in the peptide increases and decreases as the fraction of hydrophilic amino acids in the peptide increases. Just as a chemical bond can be loosely regarded as a build-up of electrons between two positively-charged nuclei, a strong 'nanoparticle–nanoparticle bond' between two metal nanoparticles with hydrophilic surfaces can be visualized as a build-up of hydrophobic amino acids between two hydrophilic spheres. This admittedly simplistic comment provides vital intuition for engineering peptides for achieving strong nanoparticle–nanoparticle bonding and does not appear to have been posited elsewhere in the literature. It was also found that in peptides which result in strong nanoparticle–nanoparticle bonds, there is a weak preference for neighboring pairs of amino acids to contain one hydrophobic and one hydrophilic or mildly hydrophobic amino acid. As described in the above discussion, the occurrence of hydrophobic–hydrophilic pairing rather than hydrophobic–hydrophobic pairs may prevent the peptides for 'folding into themselves' and not interacting with the peptide on the opposite surface. However, as the surface becomes more hydrophilic, then the preference for hydrophobic–hydrophilic pairing becomes weaker, and the occurrence of hydrophobic–hydrophobic pairs in the peptide becomes more prominent.

The observations described above and in Section 3 provide a valuable starting point for tailoring the nanoparticle–nanoparticle bond strength by careful design of peptide adsorbates. The reliability of the conclusions drawn here is directly related to the reliability of the lattice protein model and the Monte Carlo sampling technique described in Section 2. The lattice protein model has obvious deficiencies, however it provides reasonably good correlations between amino acid sequence with the stability of the folded structure [29]. For this reason, we believe that the conclusions described above are qualitatively sound and are broadly applicable. The main deficiency of the lattice protein model is that it is poor at describing the detailed shape of a folded protein, and for this reason we have avoided discussing the shape of the peptides in our simulations. In the future it may be possible to perform this study with atomistic molecular dynamics simulations, however this will first require the development of a force field which can treat both the amino acid–amino acid and variety of metal surface–amino

acid interactions simultaneously, good hardware for scanning large libraries of amino acid sequences, and good algorithms for relaxing the atomistic peptide structure on a reasonable time-scale. The Monte Carlo sampling technique employed in this study utilized the shift transformations described in Section 2. These are closely related to the 'pull' transformations used by other authors to study the lattice protein models [41]. While it is well-established that for a single 'free' (*i.e.*, not adsorbed to a surface) lattice protein, pull transformations are 'complete' (*i.e.*, are capable of scanning the entire configuration space of the model), it is currently unclear whether this holds for the current model, which considered two lattice proteins confined between two surfaces. In any case, we were unable to find any cases where a pair of configurations could not be connected *via* shift transformations, and moreover the conclusions that we drew above are physically sensible. We will therefore leave the question of the completeness of shift and pull transformations in this particular model for a future study.

Acknowledgements

This research was supported by the World Premier Research Institute Initiative promoted by the Ministry of Education, Culture, Sports, Science, and Technology of Japan (MEXT) for the Advanced Institute for Materials Research, Tohoku University, Japan, and the 'Materials for a Sustainable Energy Future' program at IPAM, University of California, Los Angeles (September–December 2013). The computation in this work was partially performed using the CX400 system RIIT at Kyushu University. Two anonymous reviewers are thanked for their suggestions.

Appendix A. Supplementary data

Supplementary data associated with this article can be found, in the online version, at doi:10.1016/j.md.2015.10.003.

References

[1] N.A. Kotov, Z. Tan, Organization of nanoparticles and nanowires in electronic devices: challenges, methods, and perspectives, in: N.A. Kotov (Ed.), Nanoparticle Assemblies and Superstructures, CRC Taylor & Francis, Boca-Raton, FL, 2006, pp. 3–73.
[2] I. Pastoria-Santos, L.M. Liz-Marzan, Tailoring the morphology and assembly of silver nanoparticles formed in DMF, in: N.A. Kotov (Ed.), Nanoparticle Assemblies and Superstructures, CRC Taylor & Francis, Boca-Raton, FL, 2006, pp. 525–550.
[3] M.J. Limo, R. Ramasamy, C.C. Perry, ZnO binding peptides, smart versatile tools for controlled modification of ZnO growth mechanism and morphology, Chem. Mater. 27 (2015) 1950–1960.
[4] M. Umetsu, M. Mizuta, K. Tsumoto, S. Ohara, S. Takami, H. Watanabe, I. Kumagai, T. Adschiri, Bioassisted room-temperature immobilization and mineralization of zinc oxide – the structural ordering of ZnO nanoparticles into a flower-type morphology, Adv. Mater. 17 (2005) 2571–2575.
[5] R.R. Naik, S.J. Stringer, G. Agarwal, S.E. Jones, M.O. Stone, Biomimetic synthesis and patterning of silver nanoparticles, Nat. Mater. 1 (2002) 169–172.
[6] S. Brown, M. Sarikaya, E. Johnson, A genetic analysis of crystal growth, J. Mol. Biol. 299 (2000) 725–735.
[7] D. de Bruyn Ouboter, T.B. Schuster, S.J. Sigg, W.P. Meier, Self-assembled peptide beads used as a template for ordered gold superstructures, Colloids Surf. B 112 (2013) 542–547.
[8] N. Yokoo, T. Togashi, M. Umetsu, K. Tsumoto, T. Hattori, T. Nakanishi, S. Ohara, S. Takami, T. Naka, H. Abe, I. Kumagai, T. Adschiri, Direct and selective immobilization of proteins by means of an inorganic material-binding peptide: discussion on functionalization in the elongation to material-binding peptide, J. Phys. Chem. B 114 (2010) 480–486.
[9] C.Y. Chiu, Y. Li, L. Ruan, X. Ye, C.B. Murray, Y. Huang, Platinum nanocrystals selectively shaped using facet-specific peptide sequences, Nat. Chem. 3 (2011) 393–399.
[10] M.M. Stevens, N.T. Flynn, C. Wang, D.A. Tirrell, R. Langer, Coiled-coil peptide-based assembly of gold nanoparticles, Adv. Mater. 16 (2004) 915–918.
[11] T. Hattori, M. Umetsu, T. Nakanishi, S. Sawai, S. Kikuchi, R. Asno, I. Kumagai, A high-affinity gold-binding camel antibody: antibody engineering for one-pot functionalization of gold nanoparticles and biointerface molecules, Bioconjugate Chem. 23 (2012) 1934–1944.
[12] S.K. Ramakrishnan, M. Martin, T. Cloitre, L. Firlej, C. Gergely, Molecular mechanism of selective binding of peptides to silicon surface, J. Chem. Inf. Model. 54 (2014) 2117–2126.
[13] M. Nonella, S. Seeger, Monitoring peptide–surface interaction by means of molecular dynamics simulation, Chem. Phys. 378 (2010) 73–81.
[14] M. Rabe, D. Verdes, S. Seeger, Understanding protein adsorption at solid surfaces, Adv. Colloid Interface Sci. 162 (2011) 87–106.
[15] D.J. Niedzwiecki, J. Grazul, L. Movileanu, Single-molecule observation of protein adsorption onto an inorganic surface, J. Am. Chem. Soc. 132 (2010) 10816–10822.
[16] M. Rabe, D. Verdes, M. Ranlk, G.R.J. Artus, S. Seeger, A comprehensive study of concepts and phenomena of the nonspecific adsorption of beta-lactoglobulin, Chem. Phys. Chem. 8 (2007) 862–872.
[17] M. Rankl, T. Ruckstuhl, M. Rabe, G.R.J. Artus, A. Walser, S. Seeger, Conformational reorientation of immunoglobin G during nonspecific interaction with surfaces, Chem. Phys. Chem. 7 (2006) 837–846.
[18] Y.F. Yano, Kinetics of protein unfolding at interfaces, J. Phys. Condens. Matter 24 (2012) 503101–503117.
[19] M. Rahman, S. Laurent, N. Tawil, L. Yahia, M. Mahmoudi, Protein–Nanoparticle Interactions, Springer, Berlin, Germany, 2013.
[20] P.C. Whitford, K.Y. Sanbonmatsu, J.N. Onuchic, Biomolecular dynamics: order–disorder transitions and energy landscapes, Rep. Prog. Phys. 75 (2012) 076601–076630.
[21] N. Go, H. Taketomi, Respective roles of short- and long-range interactions in protein folding, Proc. Natl. Acad. Sci. U. S. A. 75 (1978) 559–563.
[22] P.E. Leopold, M. Montal, J.N. Onuchic, Protein folding funnels: a kinetic approach to the sequence–structure relationship, Proc. Natl. Acad. Sci. U. S. A. 89 (1992) 8721–8725.
[23] H. Krobath, E.I. Shakhnovich, P.F.N. Faisca, Structural and energetic determinants of co-translational folding, J. Chem. Phys. 138 (2013) 215101–215111.
[24] M.A. Soler, P.F.N. Faisca, Effects of knots of protein folding properties, PLOS ONE 8 (2013) e74755–e74765.
[25] P.F.N. Faisca, R.D.M. Travasso, A. Parisi, A. Rey, Why do protein folding rates correlate with metrics of native topology, PLoS ONE 7 (2012) e35599–e35606.
[26] H. Krobath, A. Rey, P.F.N. Faisca, How determinant is N-terminal to C-terminal coupling for protein folding, Phys. Chem. Chem. Phys. 17 (2015) 3512–3524.
[27] C. Holzgrafe, A. Irback, C. Troein, Mutation-induced fold switching among lattice proteins, J. Chem. Phys. 135 (2011) 195101–195108.
[28] S. Abeln, M. Vendruscolo, C.M. Dobson, D. Frenkel, A simple lattice model that captures protein folding, aggregation, and amyloid formation, PLOS ONE 9 (2014) e85185–e85193.
[29] A. Kolinski, Lattice polymers and protein models, in: A. Kolinski (Ed.), Multiscale Approaches to Protein Modeling, Springer, NY, 2011, pp. 1–33.
[30] S.D. Chakarova, A.E. Carlsson, Model study of protein unfolding by interfaces, Phys. Rev. E 69 (2004) 021907–021916.
[31] B. Pattanasiri, Y.W. Li, D.P. Landau, T. Wurst, Wang–Landau simulations of adsorbed and confined lattice proteins, Int. J. Mod. Phys. C 23 (2012) 1240008–1240018.
[32] L.B. Wright, P.M. Rodger, S. Corni, T.R. Walsh, GolP-CHARMM: first-principles based force fields for the interaction of proteins with Au(111) and Au(100), J. Chem. Theory Comput. 9 (2013) 1616–1630.
[33] L.B. Wright, P.M. Rodger, T.R. Walsh, S. Corni, First-principles-based force field for the interaction of proteins with Au(100)(5×1): an extension of GolP-CHARMM, J. Phys. Chem. C 117 (2013) 24292–24306.
[34] H. Heinz, T.-J. Lin, R.K. Mishra, F.S. Enami, Thermodynamically consistent force fields for the assembly of inorganic, organic, and biological nanostructures: the INTERFACE force field, Langmuir 29 (2013) 1754–1765.
[35] D.B. Kokh, S. Corni, P.J. Winn, M. Hoefling, K.E. Gottschalk, R.C. Wade, ProMetCS: an atomistic force field for modeling protein–metal surface interactions in a continuum aqueous solvent, J. Chem. Theory Comput. 6 (2010) 1753–1768.
[36] A. Majzik, L. Fulop, E. Csapo, F. Bogar, T. Martinek, B. Penke, G. Biro, I. Dekany, Functionalization of gold nanoparticles with amino acid, beta amyloid peptides and fragment, Colloids Surf. B 81 (2010) 235–241.
[37] N.D. Socci, J.N. Onuchic, P.G. Wolynes, Protein folding mechanisms and the multidimensional folding funnel, Proteins 32 (1998) 136–158.
[38] M.S. Cheung, A.E. Garcia, J.N. Onichic, Protein folding mediated by solvation: water expulsion and formation of the hydrophobic core occur after the structural collapse, Proc. Natl. Acad. Sci. U. S. A. 99 (2002) 685–690.
[39] D.P. Landau, K. Binder, A Guide to Monte-Carlo Simulations in Statistical Physics, Cambridge, NY, 2009.
[40] S. Chib, E. Greenberg, Understanding the Metropolis–Hastings algorithm, Am. Stat. 49 (1995) 327–335.
[41] N. Lesh, M. Mitzenmacher, S. Whitesides, A complete and effective move set for simplified protein folding, in: T. Lengauer (Ed.), Proc. Seventh Annual Int. Conf. on Computational Molecular Biology, RECOMB, Berlin, 2003, pp. 188–201.
[42] C.J. Geyer, Importance sampling, simulated tempering, and umbrella sampling, in: S. Brooks, A. Gelman, G.L. Jones, X-L. Meng (Eds.), Handbook of Markov Chain Monte Carlo, CRC Taylor & Francis, Boca-Raton, FL, 2011, pp. 295–311.
[43] R Core Team, R: A Language and Environment for Statistical Computing. R Foundation for Statistical Computing, Vienna, Austria, 2015 http://www.R-project.org/.
[44] U. Ligges, M. Maechler, Scatterplot3d – an R package for visualizing multivariate data, J. Stat. Softw. 11 (2003) 11–20.
[45] S. Miyazawa, R.L. Jernigan, Residue–residue potentials with a favorable contact pair term and an unfavorable high packing density term, for simulation and threading, J. Mol. Biol. 256 (1996) 623–644.

[46] Y. Razvag, V. Gutkin, M. Reches, Probing the interaction of individual amino acids with inorganic surfaces using atomic force spectroscopy, Langmuir 29 (2013) 10102–10109.
[47] J.N. James, J.W. Han, D.S. Sholl, Investigation of the adsorption of amino acids on Pd(111): a density functional theory study, Appl. Surf. Sci. 301 (2014) 199–207.
[48] T. Popa, E.C.M. Ting, I. Paci, Chiral effects in amino acid adsorption on Au(111): a comparison of cysteine, homocysteine, and methionine, Surf. Sci. 629 (2014) 20–27.
[49] J.L.C. Fajin, J.R.B. Gomes, M.N.D.S. Cordeiro, DFT study of the adsorption of D-(L-)cysteine on flat and chiral stepped gold surfaces, Langmuir 29 (2013) 8856–8864.
[50] D. Costa, A. Tougerti, F. Tielens, C. Gervais, L. Stievano, J.F. Lambert, DFT study of the adsorption of microsolvated glycine on a hydrophilic amorphous silica surface, Phys. Chem. Chem. Phys. 10 (2008) 6350–6368.